Three-Dimensional Quantitative Structure−Activity Relationship Analysis of Propafenone-Type Multidrug Resistance Modulators: Influence of Variable Selection on Test Set Predictivity

Romy Fleischer and Michael Wiese*

Institute of Pharmacy, University of Bonn, An der Immenburg 4, 53121 Bonn, Germany

Received April 22, 2003

An extended set of multidrug-resistance modulators of the propafenone type were investigated using CoMFA and CoMSIA. A number of 3D-QSAR models were derived from steric, electrostatic, and hydrophobic fields and their combinations. The hydrophobic fields alone and in combination with the steric and both (steric and electrostatic) fields yielded the models with the highest cross-validated predictivity, in agreement with a previous analysis of a smaller data set of propafenone-type multidrug-resistance (MDR) modulators. Inclusion of lipophilicity did not lead to an improvement of the models. The results point to the importance of hydrophobicity as a space-directed molecular property for MDR-modulating activity. The influence of variable selection applying the GOLPE procedure was investigated with an external test set. Variable-selection procedure was repetitively applied, keeping at each stage variables with uncertain contribution to the models. For the CoMFA-based 3D-QSAR models, an increase in external prediction quality was found. In contrast, the CoMSIA-based 3D-QSAR models were not improved by the GOLPE variable-selection procedure.

Introduction

Multidrug resistance (MDR) is a major obstacle in the chemotherapeutic treatment of cancer. It is a broad-spectrum resistance to chemotherapy. Several mechanisms have been shown to lead to the MDR phenotype. The "typical" MDR is associated with the expression of P-glycoprotein (P-gp). P-gp is a membrane integrated transport protein thought to be able to recognize a large variety of cytotoxic agents as substrates for ATP-dependent efflux, thereby reducing their intracellular concentration and preventing the cytotoxic effect. P-gp-mediated MDR can be reversed by many drugs that are noncytotoxic by themselves (calcium channel blockers, antidepressants, antipsychotics, antiarrthythmics, and many others). These drugs are called MDR reversers or modulators and vary widely in their chemical structures and main biological action. Much effort has been directed to finding out the relationships between the structure and MDR reversal effect of these drugs. The most widespread hypothesis about the mechanism of action of these modulators assumes a competition between the cytotoxic agent and MDR modulator for the same binding site on P-gp.[1] However, in the past years, experimental evidence increased that indicated that there is more than one binding site for MDR modulators and cytotoxic drugs on P-gp.[2] Thus, 3D-QSAR analysis of structural features important for MDR reversal activity should be restricted to compounds that presumably bind to the same binding site of P-gp.

Some years ago, we performed the first 3D-QSAR analysis of MDR modulators. In those studies, two large classes of modulators were investigated, namely, propafenones[3] and phenothiazines and related compounds.[4] By use of the CoMFA approach, highly predictive models were obtained in both cases; however, the number of compounds and their structural variety were limited. For this reason, we continued our investigation as new data for propafenone derivatives became available. The aim of this study was severalfold: to develop a new 3D-QSAR model based on an expanded data set and to compare the results with those from our earlier study, to test the predictivity of the models on a larger and more heterogeneous test set, and to study the effect of variable selection on predictivity for an external test set.

Additionally we compared the traditional CoMFA with the CoMSIA approach. The latter has been claimed to be better interpretable and to give results comparable to results from CoMFA.[5]

The GOLPE procedure has been shown to lead to 3D-QSAR models with better internal predictions by selecting the most informative field regions and minimizing redundant information.[6−10] However, the influence of this variable-selection procedure on external predictivity for a test set has rarely been reported. Therefore, the effect of these data pretreatment on predictive power both for the cross-validation and the external test set was investigated in detail.

Results and Discussion

The results for CoMFA models derived from the training set of 48 MDR modulators (compounds **1**−**48** in Table 1) are presented in Table 2, and those for the corresponding CoMSIA models are in Table 3. Models were calculated for each field alone and in combination with the other fields. The maximum number of components to be included in the first cross-validated run was set to 14 and increased if necessary to yield the model with the highest Q^2. Several local optima of $SDEP_{cv}$ for some of the models with a high number of optimal

* To whom correspondence should be addressed. Phone: + 49 228 73 5212. Fax: +49 228 737929. E-mail: mwiese@uni-bonn.de.

10.1021/jm030876r CCC: $25.00
Published on Web 10/09/2003

Table 1. Structures, MDR Reversal Activities, and Calculated logP Values of the Investigated Propafenone-Type MDR Modulators

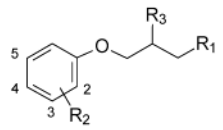

Compound	R_1	R_2 in 2	R_3	IC_{50} [μM]	$logP_{Molgen}$	$logP_{HINT}$
1	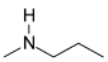	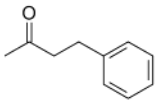	—OH	1.08	3.36	3.99
2		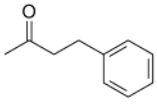	—OH	0.68	3.67	5.05
3	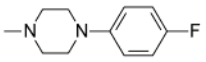	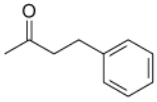	—OH	0.14	4.93	6.41
4	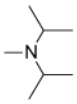	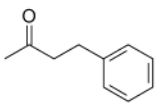	—OH	0.31	4.25	4.66
5	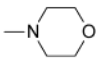	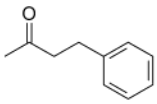	—OH	3.75	2.54	3.95
6	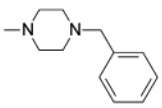	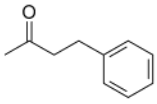	—OH	0.38	4.43	6.06
7	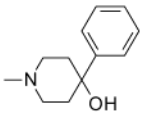	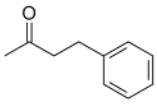	—OH	0.07	3.98	5.03
8	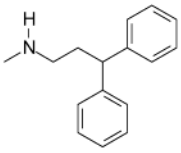	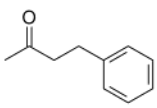	—OH	0.72	6.51	6.96
9		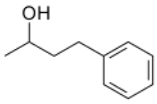	—OH	1.34	3.94	4.28
10	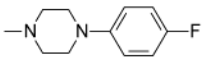	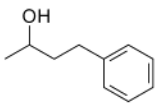	—OH	0.67	5.20	5.64
11	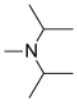	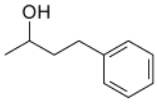	—OH	1.74	4.52	3.90
12	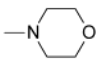	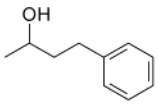	—OH	9.54	2.81	3.19
13		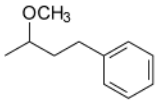	—OH	0.77	4.30	4.89

Table 1 (Continued)

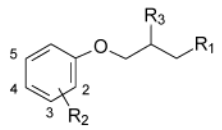

Compound	R_1	R_2 in 2	R_3	IC_{50} [μM]	$logP_{Molgen}$	$logP_{HINT}$
14	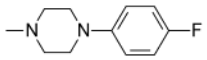	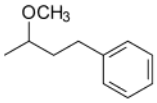	—OH	0.23	5.56	6.25
15	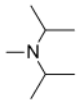	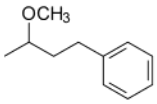	—OH	0.66	4.88	4.51
16	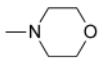	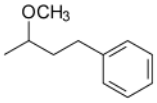	—OH	1.80	3.17	3.80
17	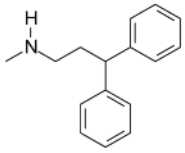	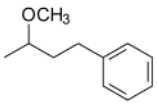	—OH	0.75	7.14	6.81
18	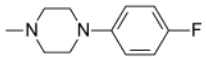	—$COCH_3$	—OH	3.84	2.67	4.32
19	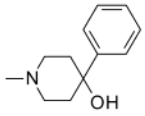	—$COCH_3$	—OH	2.83	1.73	2.94
20		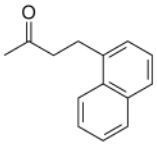	—OH	0.17	4.67	6.21
21	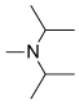	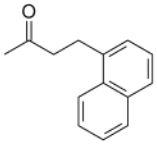	—OH	0.54	5.25	5.82
22	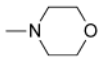	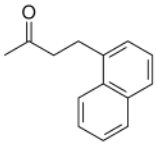	—OH	0.68	3.54	5.11
23	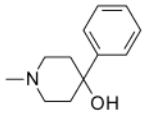	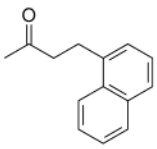	—OH	0.07	4.98	6.19
24	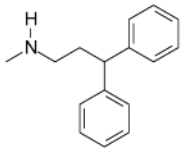	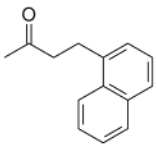	—OH	0.72	7.51	8.12
25		—$COCH_2CH_3$	—OH	6.84	2.07	3.50

Table 1 (Continued)

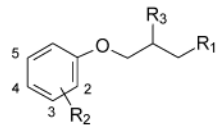

Compound	R_1	R_2 in 2	R_3	IC_{50} [μM]	$logP_{Molgen}$	$logP_{HINT}$
26	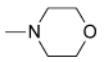	—$COCH_2CH_3$	—OH	207.2	0.94	2.40
27	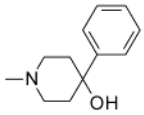	—$COCH_2CH_3$	—OH	0.30	2.38	3.48
28	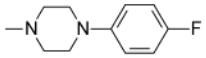	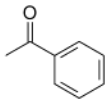	—OH	0.42	4.57	6.58
29	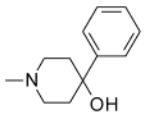	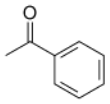	—OH	0.19	3.62	5.20
30		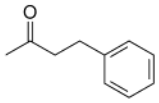 b)	—OH	1.36	3.67	4.66
31	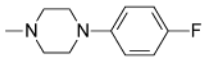	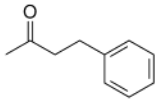 b)	—OH	2.53	4.93	5.79
32	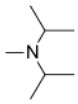	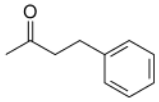 b)	—OH	0.92	4.25	4.27
33	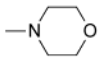	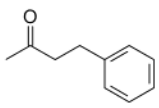 b)	—OH	6.86	2.54	3.56
34	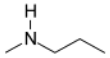	—OH c)	—OH	3.02	3.00	3.45
35		—OH c)	—OH	2.30	3.29	4.50
36	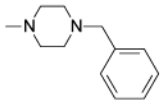	—OH c)	—OH	0.53	4.04	5.51
37	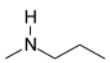	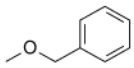 c)	—OH	0.11	5.00	5.61
38		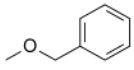 c)	—OH	0.17	5.28	6.67
39	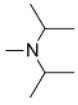	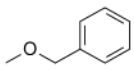 c)	—OH	0.08	5.86	6.28
40	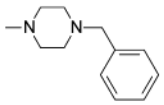	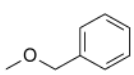 c)	—OH	0.12	6.04	7.68

Table 1 (Continued)

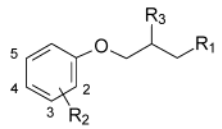

Compound	R_1	R_2 in 2	R_3	IC_{50} [μM]	$logP_{Molgen}$	$logP_{HINT}$
41		—$COCH_3$ b)	—OH	75.9	1.42	2.57
42	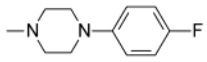	b) —$COCH_3$	—OH	11.89	2.67	3.93
43	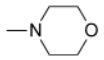	—$COCH_3$ b)	—OH	302.05	0.28	1.47
44		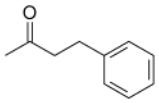 a)	—OH	0.39	3.67	4.81
45	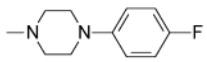	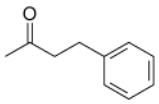 a)	—OH	1.12	4.93	6.17
46		—$COCH_3$ a)	—OH	9.07	1.42	2.72
47	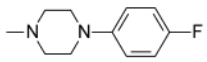	—$COCH_3$ a)	—OH	11.36	2.67	4.08
48	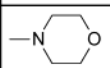	—$COCH_3$ a)	—OH	117.69	0.28	1.62
t_1b	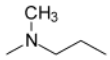	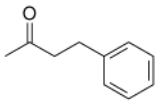	—OH	0.49	3.77	4.74
t_1c		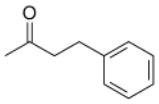	—OH	2.64	2.94	3.66
t_1d	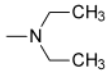	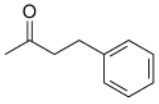	—OH	0.91	3.62	4.74
t_1f	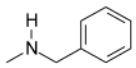	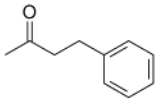	—OH	0.76	4.30	4.46
t_1g		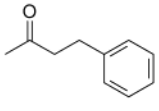	—OH	1.82	3.26	4.47
t_3c	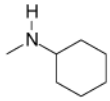	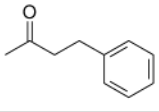	—OH	0.34	4.11	5.20
t_1l	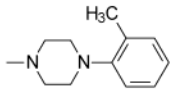	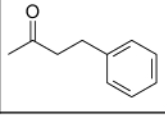	—OH	0.05	5.26	6.93

Table 1 (Continued)

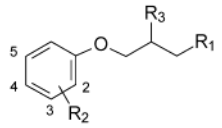

Compound	R_1	R_2 in 2	R_3	IC_{50} [μM]	$logP_{Molgen}$	$logP_{HINT}$
t_3f	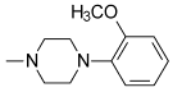	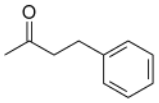	—OH	0.11	4.89	6.62
t_3g	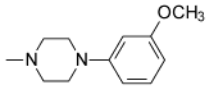	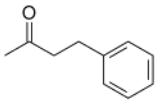	—OH	0.12	4.65	6.43
t_1k	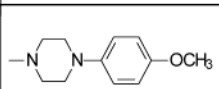	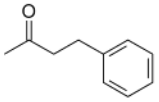	—OH	0.18	4.65	6.32
t_3i	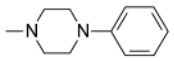	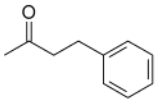	—OH	0.21	4.25	6.39
t_5a	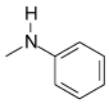	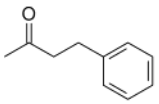	—OH	6.47	4.23	4.66
t_5b	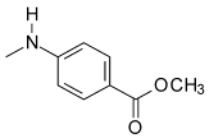	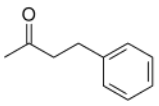	—OH	2.53	4.05	4.52
t_6a	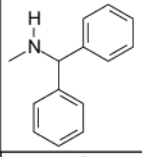	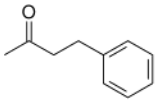	—OH	1.02	6.01	5.79
t_6b	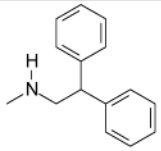	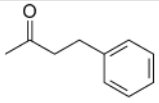	—OH	0.09	6.16	6.33
t_6c	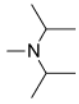	—OH [c]	—OH	1.04	3.87	4.12

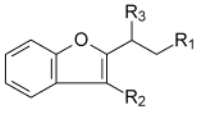

compound	R_1	R_2	R_3	IC_{50} [μM]	$logP_{Molgen}$	$logP_{Hint}$
t_2a	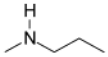		—OH	438.65	3.10	2.38
t_2b	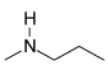	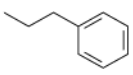	—OH	58.14	4.07	3.93

Table 1 (Continued)

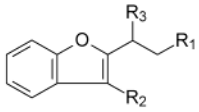

compound	R_1	R_2	R_3	IC_{50} [μM]	$logP_{Molgen}$	$logP_{Hint}$
t_2c	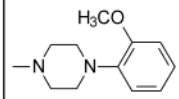	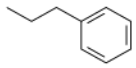	—OH	0.88	5.32	6.42
t_2d	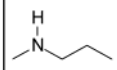	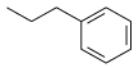	—H	8.56	4.71	4.75
t_2e	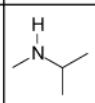	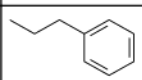	—H	20.19	4.54	4.53
t_2f	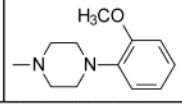	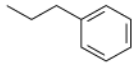	=O	16.63	5.05	6.94

[a] R_2 in position 3. [b] R_2 in position 4. [c] R_2 in position 4 and additionally a 3-phenylpropanoyl group in position 2.

Table 2. Summary of Cross-Validated Q^2 Values Obtained with the Different CoMFA Fields and Their Combinations[a]

	cross-validated Q^2	
field(s)	LOO	random groups
S	0.801	0.760
E	0.780	0.731
H	0.810	0.772
Ho	0.795	0.750
S & E	0.817	0.784
B	0.806	0.780
S & H	0.836	0.788
S & Ho	0.807	0.763
E & H	0.818	0.763
E & Ho	0.806	0.759
S & E & H	0.830	0.789
S & E & Ho	0.817	0.778
B & H	0.819	0.788
B & Ho	0.801	0.768

[a] Abbreviations: S (steric); E (electrostatic); H (HINT); Ho (HINT, hydrophobic only); B (both standard CoMFA fields).

Table 3. Summary of Cross-Validated Q^2 Values Obtained with the Different CoMSIA Fields and Their Combinations[a]

	cross-validated Q^2	
field(s)	LOO	random groups
S	0.699	0.695
E	0.714	0.622
H	0.806	0.788
S & E	0.769	0.747
S & H	0.796	0.776
E & H	0.802	0.779
S & E & H	0.788	0.772

[a] Abbreviations: S (steric), E (electrostatic), H (hydrophobic) CoMSIA fields.

components (ONC) as judged by Q^2 were found. In these cases Q^2 increased slowly but steadily with the number of considered latent variables, reaching its optimum at a rather high number of latent variables. However, the increase in Q^2 was less than 0.01 in most cases when compared to the ONC that yielded the lowest SDEP.

Table 4. Summary of Cross-Validated Q^2 Values Obtained with the Different CoMFA Fields and Their Combination with Lipophilicity Variables[a]

	cross-validated Q^2	
field(s)	LOO	random groups
S & logP	0.797	0.777
E & logP	0.815	0.797
S & HlogP	0.828	0.809
E & HlogP	0.854	0.843
H & HlogP	0.856	0.849
B & logP	0.824	0.814
B & HlogP	0.797	0.771

[a] Abbreviations: S (steric); E (electrostatic); H (HINT); B (both standard CoMFA fields); logP ($logP_{Molgen}$ listed in Table 1); HlogP ($logP_{HINT}$ Listed in Table 1).

Therefore, for the variable-selection procedure, ONC was selected on the basis of the number of components yielding the lowest $SDEP_{cv}$.

In both cross-validation schemes, the HINT hydrophobic field (H) yielded the best CoMFA models among those derived from single fields, with the electrostatic field giving the worst model and the steric and hydrophobic only field (Ho) lying in between (Table 2). This result is in agreement with the results of our previous CoMFA studies of propafenone-type MDR modulators. For the smaller data set investigated in ref 3, the HINT hydrophobic only field yielded the best cross-validated model, followed by the HINT field, and the electrostatic field always gave models with the lowest predictivity as measured by Q^2. For the previously investigated smaller data set, this difference was even more pronounced. One difference was the relative performance of the hydrophobic and hydrophobic only fields. For the larger data set investigated now, the Ho field was always worse than the standard HINT field, pointing to the possible role of hydrophilic/ampiphilic interactions that were not apparent in the smaller data set. However, each field led to very satisfactory models with

rather high Q^2 values. Therefore, all fields seem to include information relevant for the description of the activity differences among the investigated derivatives.

In a comparison of the CoMFA-derived models with the corresponding CoMSIA ones, it is obvious that the CoMFA methodology gives models with considerably higher Q^2 and lower $SDEP_{cv}$ values (cf. Tables 2 and 3) except for the hydrophobic field, where the difference is small in the case of LOO and CoMSIA performs slightly better in case of random group leave out.

Combining two fields increased Q^2 despite the relative high values already obtained with single fields. This indicates partly different information captured by the fields. Again, models containing the hydrophobic field were the best, especially the combination with the steric field, as found before for the smaller set of propafenone derivatives. The combination of steric and electrostatic fields that contain additional points with limit values (±30 kcal/mol) slightly outperformed the B field; however, it became worse after variable selection (see below). Therefore, these points seem to introduce noise into the model that cannot be removed by the variable-selection procedure. For the CoMSIA models, the combination of steric and electrostatic fields increased Q^2 considerably (Table 3). However, the addition of the steric or electrostatic field to the hydrophobic one did not lead to an improvement. Finally, combining all three types of fields did not further increase the internal predictive power.

Total lipophilicity, though explaining about 50% of the variance, did not contribute much to the quality of the CoMFA models, but the differences in Q^2 between LNO and LOO cross-validations were halved and corresponded to those of the CoMSIA models (Table 4). The strongest effect was observed for the electrostatic field that gave the worst model. By addition of $logP_{Molgen}$ or especially HlogP, its internal predictivity was greatly enhanced (compare Tables 2 and 4). Also, the combination of the Hint field and Hint-logP did not lead to a significant improvement. This was tested because logP should capture the general lipophilicity, while the Hint field represents the spatial arrangement of hydrophobic properties. But again, this combination gave the best model among those that included lipophilicity as an additional scalar variable. The differences between the models derived either from logP or from Hint-logP was small, Hint-logP yielding the better ones, when combined with single fields. Because the effect of scalar lipophilicity descriptors on the quality and stability of the models was small, the other combinations were not calculated further.

Variable Selection. Variable selection did not reduce the number of latent variables necessary to obtain the highest Q^2 value in most cases, or it reduced the number only slightly by 1. Before variable selection, the optimal number of components determined via the highest Q^2 and the lowest SDEP (calculated according to SYBYL CoMFA) were equal or differed by 1 only (data not shown).

After the first run of variable selection, Q^2 was increased by ca. 0.05 in most cases (Figures 1 and 2). Repeated application of fractional factorial design (FFD) led to a further increase of Q^2 that became smaller with each repetition. It seemed that a maximal Q^2 was asymptotically reached, the level depending on the quality of the starting model. However, in a few cases (CoMFA and CoMSIA steric fields alone), the third FFD led to a decrease in Q^2.

The number of "fixed" variables that was found by FFD to positively contribute to the cross-validated predictive power varied during the FFD runs and generally decreased from the first to the third run. This shows that the judgment of a variable to positively contribute to the model is very much dependent on the presence of other X variables and underlines the importance of keeping "uncertain" variables.

Again, Hint was the best single field, and the difference in Q^2 in comparison to the other fields was increasing (Figure 1). When Q^2 values from LOO and LNO are compared, a stabilizing effect of the GOLPE variable selection became apparent. Before fractional factorial design based selection, the differences were on average 0.04 and decreased to 0.02 after the second FFD run.

Also, CoMFA models combined with logP were subjected to variable selection. Though the same trends were observed in general, the increase in Q^2_{LOO} and especially in Q^2_{LNO} was much less pronounced for the combination of single fields and logP or HlogP. For the Both field, HlogP performed worse than logP, but the difference was greatly reduced after the first run of variable selection (Figure 2).

From the relatively large number of omitted compounds (eight per run) and the low standard deviation of the SDEP values (about 10% of SDEP), it could be estimated that the models should have good predictive power.

For the CoMSIA models, the difference in Q^2 between LOO and LNO was even lower for most models (Figure 3), pointing to the fact that LOO is more overoptimistic especially in the case of CoMFA-derived models. Also, for CoMSIA models, qualitatively the same behavior was observed; the first run of the variable-selection procedure led to an increase in Q^2 of about 0.05, while repetition of variable selection yielded smaller increases in Q^2. Thus, the models derived from either the CoMFA fields or the CoMSIA fields behaved similarly in terms of internal predictivity. However, the effect of the second and third FFD run on internal predictivity was smaller for the CoMSIA-derived models. Inspection of the number of removed field variables showed that the first FFD run eliminated usually between 20% and 30% of the initial field variables from both kind of fields, while the effects of the second and third FFD were smaller and differed for the CoMFA and CoMSIA fields. For the same fields and field combinations, the second FFD reduced the number of X variables about 2 times more for the CoMFA fields than for the CoMSIA fields. And this discrepancy was even more pronounced for the third FFD that eliminated only a few percent of the X variables in the case of CoMSIA fields. This could be attributed to distribution of the values of the property fields. In the CoMSIA approach, the potentials that create the fields are much "softer" than in CoMFA and elimination of irrelevant variables seems to be easier for the GOLPE algorithm than in the case of CoMFA. In the case of the CoMSIA fields, considerably less irrelevant variables remained after the first FFD run;

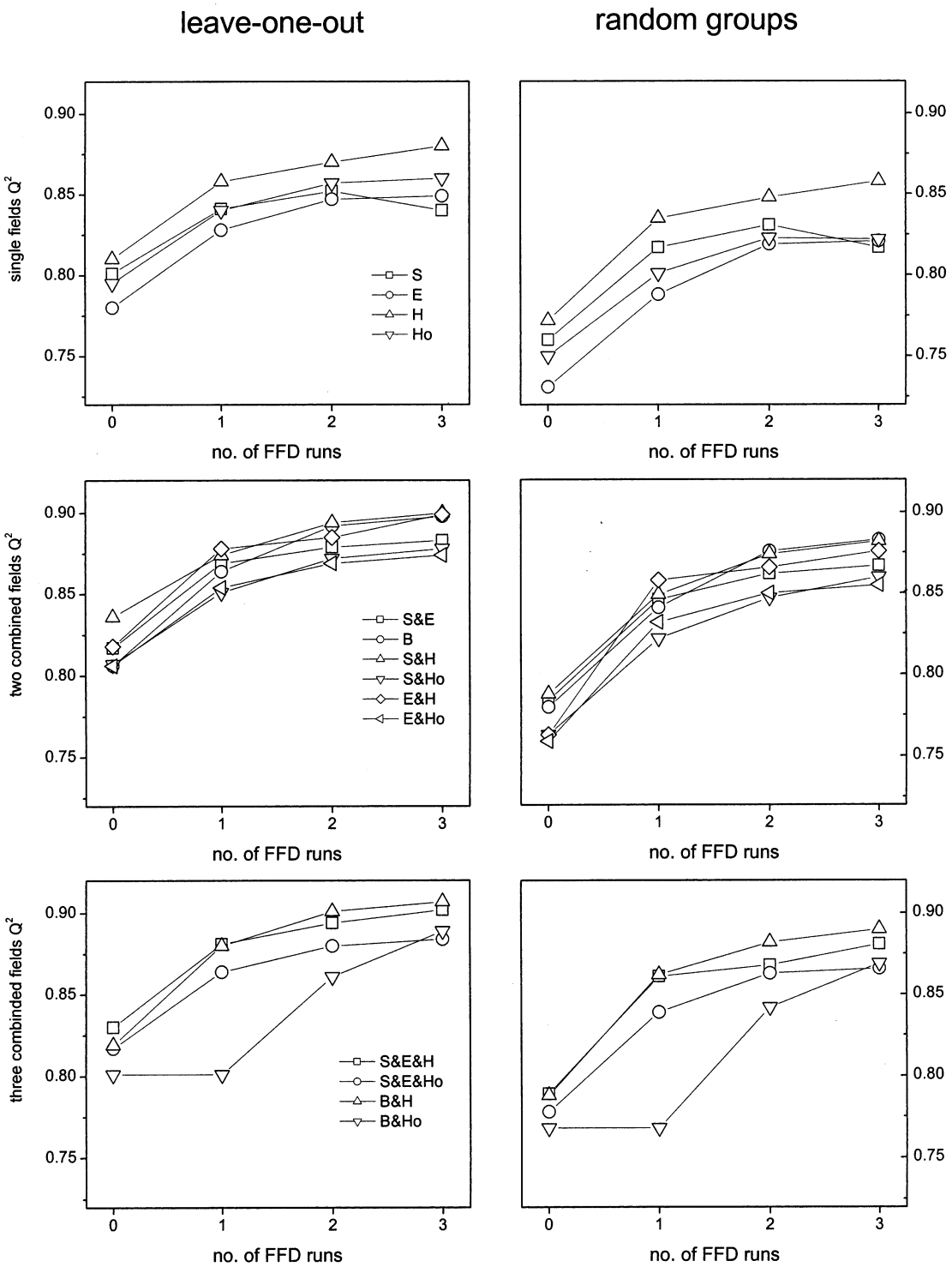

Figure 1. Summary of cross-validated Q^2 values obtained with different CoMFA fields after different runs of variable selection by FFD. Shown on the left are Q^2 values from the leave-one-out procedure, and on the right are those from random group leave out. Abbreviations are the following: S (steric), E (electrostatic), H (HINT), Ho (HINT, hydrophobic only), B (both standard CoMFA fields).

thus, it is expected that further elimination of a few irrelevant variables will change the result to a lesser extent as in CoMFA.

External Predictivity. Because the GOLPE procedure is based on Q^2, e.g., internal predictivity of the training set, it was of interest to study how it influenced the prediction of an external test set. This kind of prediction is far more important for the design of new compounds. Therefore, we compared the cross-validation results with those of the test set in detail.

Inspection of the test set predictions as a function of the number of latent variables revealed that internal and external predictivity was not much related. A local or even a global maximum in predictivity occurred, with two latent variables (Figure 4). This maximum was shifted to three latent variables when logP or HlogP was additionally included. This is in agreement with observations made by others that more robust models with respect to external predictivity are obtained with a smaller number of latent variables. The same tendency

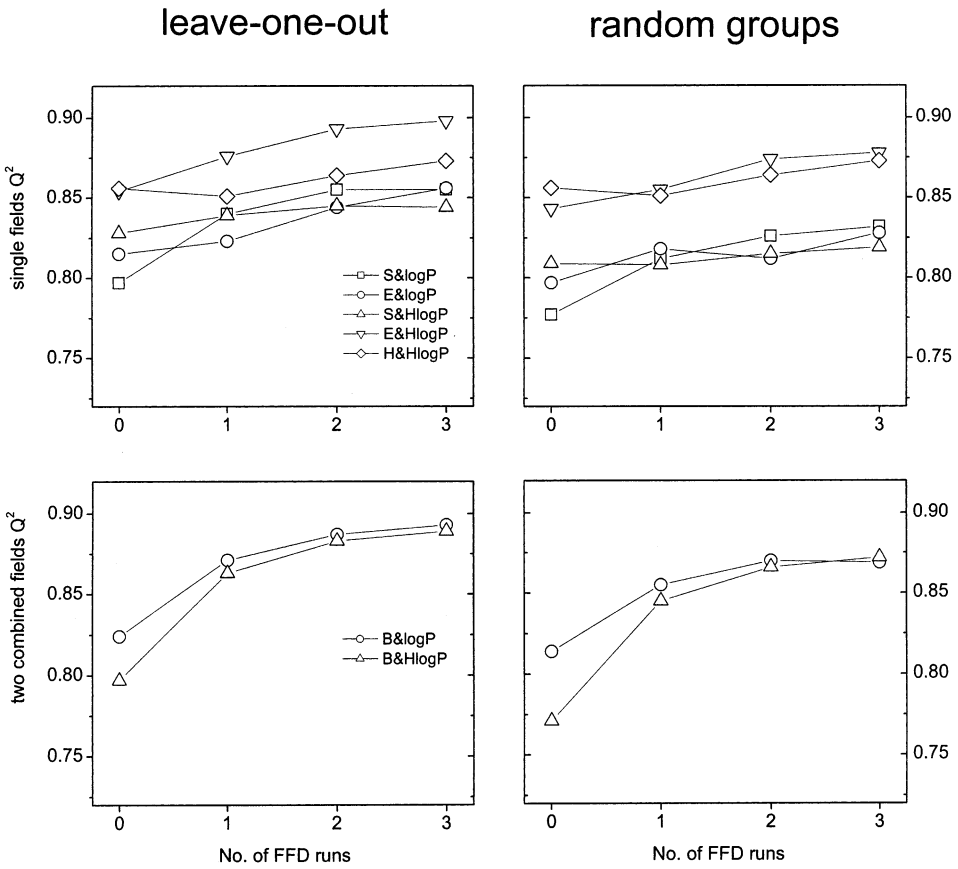

Figure 2. Summary of cross-validated Q^2 values obtained with different CoMFA fields and their combination with lipophilicity variables after different runs of variable selection by FFD. Shown on the left are Q^2 values from the leave-one-out procedure, and on the right are those from random group leave out. Abbreviations are the following: S (steric), E (electrostatic), H (HINT), B (both standard CoMFA fields), logP ($logP_{Molgen}$ listed in Table 1), HlogP ($logP_{HINT}$ listed in Table 1).

was observed when the newly introduced figure of merit P^2 was used (Figure 5). When Figures 4 and 5 are compared, it can be seen that P^2 yielded higher values, a fact that was observed in all cases and that can be attributed to the differences of the mean and standard deviation between training and test sets (mean was 5.89 vs 6.14 and SD was 0.87 vs 0.67 for training and test sets respectively). Thus, P^2 is to be preferred if the mean values of the training and test sets differ.

To compare the predictivity of the different fields and variable-selection steps, the optimal number of components as determined by random group selection from the training set was used. Thus, not the "best" Q^2 and P^2 results were used, as can be seen from Figures 4 and 5, where the maximum was at five latent variables. This was done as in a real test; no prior information about the number of latent variables to be chosen is available. In the prediction process, those compounds that were mispredicted by more than two standard deviations of the cross-validated training set model were considered to be outliers.

When the performance on the training and the test sets was compared, the order changed in the case of single fields. While the HINT field gave the best model according to cross-validation for up to three FFDs (Figure 1), with the order H > S > Ho ∼ E, the steric field yielded the best overall prediction (order: S > Ho > H ≫ E). This difference was mainly due to three compounds (those activities were underestimated by about 1 log unit using the hydrophobic field), namely, compounds **t_1l**, **t_6b**, and **t_2c** (Table 5). The first two of these three were also underpredicted in the case of the other fields, though to a lesser extent. Compound **t_1l** was the most active one of the whole data set; thus, its correct prediction required an extrapolation out of the activity range. Compound **t_6b**, which possesses a diphenylmethyl moiety, was more active (by about 1 order of magnitude) than compounds with the same moiety present in the training set (**8**, **17**, **24**). And compound **t_2c** was a benzofurane derivative that showed the highest activity in this series, being more active than a similar derivative (**t_2f**) by a factor of about 20.

When combinations of different fields were used to build the CoMFA models, a different behavior was observed in the prediction process. The combinations involving the hydrophobic field proved to be superior to the others, leading to the highest R^2_{pred} and P^2 values for the external test set.

The inclusion of total lipophilicity as an additional independent variable led to somewhat different results. While the overall predicitivity was not or only moderately improved, the two compounds that were found to be outliers in all cases (**t_1l**, **t_6b**) were now much better predicted (Table 6). This can be attributed to their high calculated logP values that lie in the uppermost range of the training set. When two fields were combined, the cross-validation results were improved (cf. Figure 1), with the standard Both or steric and hydrophobic fields giving the best models. The same ranking was observed

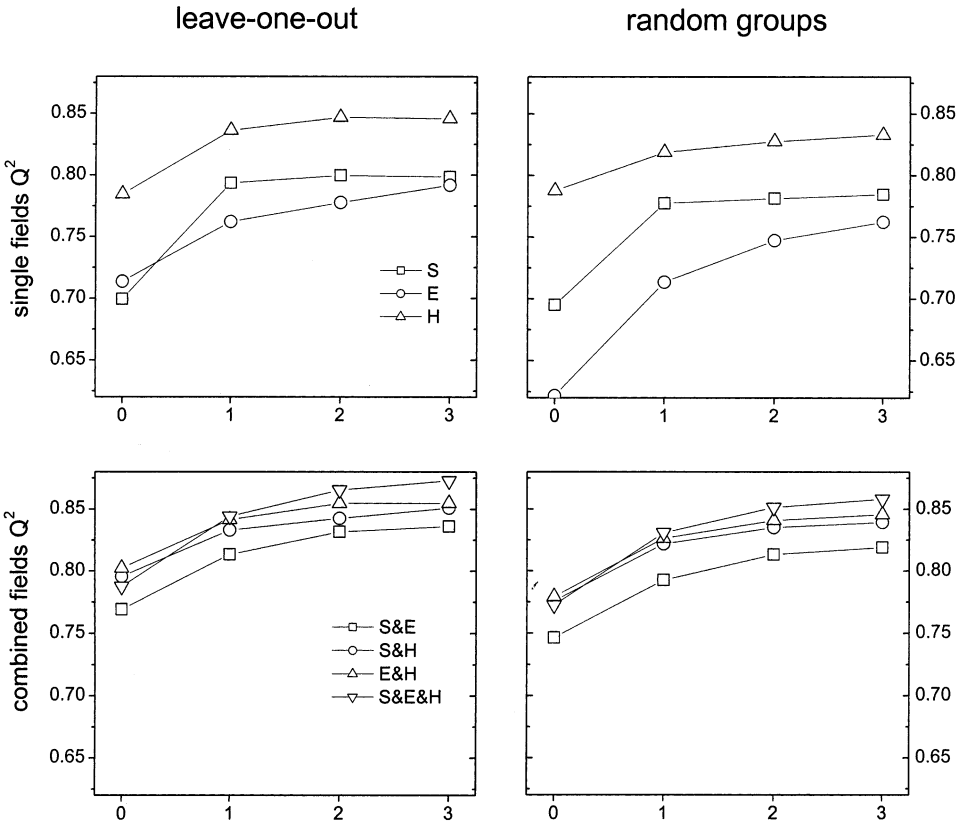

Figure 3. Summary of cross-validated Q^2 values obtained with different CoMSIA fields after different runs of variable selection by FFD. Shown on the left are Q^2 values from the leave-one-out procedure, and on the right are those from random group leave out. Abbreviations are the following: S (steric), E (electrostatic), H (hydrophobic) CoMSIA fields.

for the external predictions, where the combination of steric and hydrophobic fields yielded the best result ($P^2 \approx 0.70$), followed by the Both fields ($P^2 \approx 0.63$). Also, in this case, inclusion of lipophilicity led to a minor improvement in P^2 only.

The effect of variable selection by repeated FFD runs was not fully consistent among the models derived from different fields and combinations of them, but a general trend could be observed. The R^2_{pred} increased after the first run of variable selection in almost all cases, while the effects of the second and third run differed (Table 5). In some cases, such as the combination of steric and hydrophobic HINT fields, a steady increase in R^2_{pred} occurred, while in most cases the influence on R^2_{pred} was small, either increasing or decreasing it very slightly as in case of the steric field (Figure 4, Table 5). Also, differences in the behavior of P^2 and R^2_{pred} were observed. The influence of the variable selection on P^2 was generally not as strong as in case of R^2_{pred}. This could be explained by the observation that the outliers became mostly better predicted with increasing runs of the variable selection process (Table 5).

For the CoMSIA-derived models, similar results were obtained. Again, in most cases, a maximum in external predictivity occurred with two components. This is followed by a second maximum in the range of 5−10 components, 10 being the maximum of latent variables that were considered. There was one noticeable exception. The combination of steric plus electrostatic field yielded a nearly perfect prediction prior to variable selection, with a R^2_{pred} and P^2 of 0.95 (Figure 6). This must be regarded as chance result because Q^2 was much lower for the training set. The first run of variable selection decreased P^2 and R^2_{pred} to values in the range observed for the other models with good predictivity, and the second run led to an increase in P^2.

The hydrophobic field that led to the best model (Figure 2) yielded also the best external predictions, considering single fields, followed by the steric field, while predictions based on the electrostatic field alone were clearly worse with negative R^2_{pred} and P^2 values. This was in contrast to CoMFA-derived models, where the hydrophobic field yielded the best model but led to poorer predictions than the steric field.

From a comparison of the combined fields, the combination of all three fields led to the best predictions, followed by the combination of steric plus hydrophobic fields (Figure 6).

The outliers in the predictions were mostly similar to those of the CoMFA-derived models (Table 7). Again, compound **t_1l** with the highest activity was poorly predicted by all models except the one based on the steric field alone. Compound **t_6a** was overpredicted when the hydrophobic field alone or in combination with the steric one had been used to generate the CoMSIA model. When the steric field derived model for prediction was used, compounds **t_2c** and **t_2d** were consistently outliers whose activities were underestimated (Table 7). **t_2c** was also found to be an outlier in most of the CoMFA-derived predictions.

The effect of variable selection on external predictivity differed somewhat for the CoMSIA-derived models. In all cases, a slight (0.01−0.02) to moderate (by 0.07) decrease in P^2 occurred after the first run of variable selection (with the exception of the combination of steric plus electrostatic field, were the decrease was 0.36 due

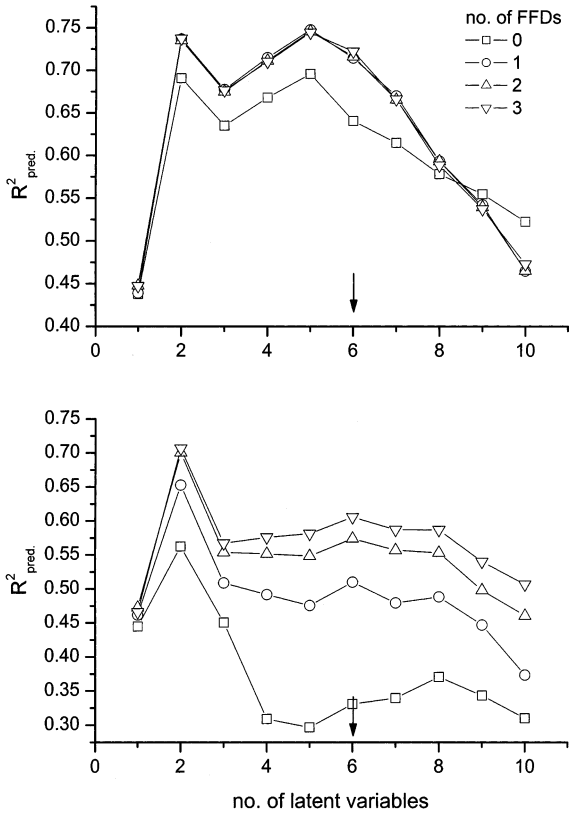

Figure 4. Influence of the number of latent variables on external predictivity as measured by R^2_{pred}. Shown are two representative examples: (top) steric CoMFA field; (bottom) combination of steric and HINT fields. The arrow indicates the optimal number of latent variables (6) as obtained from random group leave out statistics.

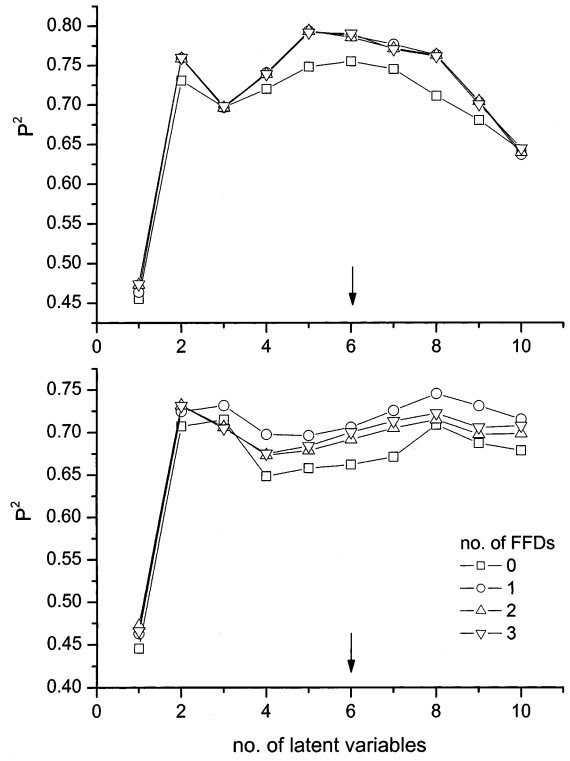

Figure 5. Influence of number of latent variables on external predictivity as measured by P^2. Shown are the same fields as in Figure 4: (top) steric CoMFA field; (bottom) combination of steric and HINT fields. The arrow indicates the optimal number of latent variables (6) as obtained from random group leave out statistics.

to the perfect prediction occurring by chance). But the continuation of the variable-selection process mostly led to a returned increase that exceeded the decrease considerably for the model with the best predictivity (steric + electrostatic + hydrophobic field), while for others approximately the same P^2 and R^2_{pred} values as without variable selection were reached or slightly exceeded after the second run of variable selection (Figure 6). The third FFD run led generally to a (small) decrease in P^2 and R^2_{pred}.

When the predictions obtained from the CoMFA and CoMSIA models were compared, the latter ones were less dependent on the field chosen. With the exception of the electrostatic field, which gave negative R^2_{pred} and P^2 values, the other fields and their combinations led to predictions with similar P^2 in the range 0.56−0.68, with the exception of the best combination (steric + electrostatic + hydrophobic: 0.77). The differences for the CoMFA-derived models were somewhat larger, again with the electrostatic field leading to a far worst prediction when used alone. For the other fields, P^2 was ranging from 0.47 for the hydrophobic field to 0.79 for the steric field.

Conclusion

For the CoMFA fields derived models, the variable selection increased not only internal predictions but also the external predictivity for the test set. A second application of the FFD variable selection led either to a further slight increase in prediction quality or did not change it. A further run of the variable selection did not change the predictivity for the test set, or it slightly decreased the predictivity in some cases. Thus, one or two rounds of variable selection seem to be advantageous, while a too strong variable selection leads to overfitting and poorer external predictions.

In contrast, for CoMSIA-derived models, variable selection improved the cross-validation results but did not lead to an improvement of the predictions for the external test set. For only the best model that was based on all three fields, a significant improvement was obtained after the second FFD run. This difference in behavior could be due to the differences in the field variables. In CoMFA, interactions with a probe are collected outside the molecules, while in CoMSIA, the similarity at and near the atomic positions is calculated and used in the 3D-QSAR. Of course, further studies must be undertaken to investigate whether this trend that was observed is a more general one.

Experimental Section

Compounds and Biological Activity Data. Data on MDR reversing activity in vitro in the CCRF-CEM/VCR-1000 cell line resistant to vincristine were collected from papers of Ecker and co-workers.[11−15] A total of 70 compounds were available for analysis. In these papers, three different measures of MDR reversal activity had been applied: MTT assay of daunomycin cytotoxicity, inhibition of rhodamine-123 efflux, and inhibition of daunomycin efflux. Because inhibition of daunomycin efflux is the most direct measure of P-gp modulating activity and had been determined for most of the compounds, it was selected as a measure of biological activity. When the reported activity values were compared, it was noted that the activity values of several derivatives in ref 14 differed from those

Table 5. Predictions for the External Test Set by Different CoMFA Models before (0) and after 1−3 FFD Runs[a]

		steric				HINT				steric & HINT				Both				Both & HINT			
compd	obsd	0 FFD	1 FFD	2 FFD	3 FFD	0 FFD	1 FFD	2 FFD	3 FFD	0 FFD	1 FFD	2 FFD	3 FFD	0 FFD	1 FFD	2 FFD	3 FFD	0 FFD	1 FFD	2 FFD	3 FFD
t_1b	6.314	6.006	5.984	6.002	5.996	5.967	5.954	6.026	6.034	5.946	6.035	6.091	6.117	6.077	6.118	6.088	6.125	6.182	6.280	6.220	6.175
t_1c	5.577	5.353	5.384	5.392	5.390	5.705	5.698	5.752	5.765	5.572	5.734	5.788	5.784	5.868	6.004	5.985	6.008	6.054	6.072	6.005	5.995
t_1d	6.042	5.923	5.993	6.001	5.995	5.955	5.962	5.991	5.968	5.801	5.816	5.902	5.918	6.041	6.084	6.082	6.097	6.115	6.178	6.104	6.088
t_1f	6.602	6.311	6.310	6.318	6.310	6.109	6.088	6.155	6.133	5.908	6.041	6.097	6.110	5.830	**5.893**	**5.903**	**5.895**	5.988	6.116	6.036	**5.992**
t_1g	5.740	5.787	5.795	5.804	5.802	5.946	5.943	5.969	5.936	5.735	5.748	5.799	5.822	6.050	6.137	6.137	6.169	6.132	6.192	6.111	6.113
t_1k	6.745	6.616	6.602	6.605	6.607	6.399	6.422	6.414	6.380	6.472	6.474	6.565	6.605	6.360	6.490	6.491	6.481	6.369	6.679	6.635	6.652
t_1l	7.301	6.666	6.649	6.655	6.653	**6.297**	**6.366**	**6.354**	**6.276**	**6.391**	**6.413**	**6.525**	**6.560**	6.626	6.737	6.720	6.714	**6.476**	6.816	6.783	6.770
t_3c	6.469	5.763	5.861	5.872	5.867	5.707	5.760	5.867	5.801	**5.545**	**5.593**	**5.543**	**5.572**	6.059	6.213	6.160	6.181	5.989	6.077	5.998	5.924
t_3f	6.956	6.775	6.773	6.778	6.776	6.483	6.522	6.508	6.436	6.613	6.640	6.743	6.779	6.380	6.457	6.454	6.473	6.436	6.779	6.751	6.750
t_3g	6.921	6.673	6.671	6.675	6.677	6.269	6.301	6.341	6.261	6.408	6.424	6.496	6.521	6.397	6.416	6.417	6.409	6.362	6.654	6.613	6.622
t_3i	6.678	6.634	6.625	6.628	6.627	6.588	6.616	6.606	6.537	6.513	6.502	6.606	6.633	6.653	6.751	6.742	6.738	6.539	6.910	6.878	6.867
t_5a	5.189	5.663	5.693	5.706	5.698	5.685	5.697	5.782	5.761	5.510	5.596	5.642	5.668	5.786	5.801	5.766	5.806	5.802	5.780	5.691	5.673
t_5b	5.597	5.623	5.648	5.663	5.659	5.914	5.816	5.875	5.882	5.689	5.717	5.824	5.854	5.661	5.657	5.624	5.668	5.828	5.826	5.749	5.766
t_6a	5.991	6.161	6.224	6.238	6.233	6.106	6.101	6.172	6.121	5.821	6.000	6.036	6.058	5.808	5.965	5.951	5.966	5.964	6.065	6.014	5.982
t_6b	7.046	6.446	6.413	6.421	6.423	**6.034**	**6.064**	**6.105**	**6.046**	**6.007**	**6.264**	**6.292**	**6.329**	**6.002**	**6.031**	**6.018**	**6.067**	**6.123**	**6.250**	**6.193**	**6.210**
t_6c	5.983	6.162	6.251	6.256	6.248	5.931	5.925	6.014	6.016	5.882	5.977	6.044	6.052	6.128	6.213	6.173	6.223	6.057	6.201	6.112	6.123
t_2a	4.752	4.842	4.720	4.711	4.718	4.895	5.129	5.105	5.161	4.648	4.786	4.869	4.877	4.872	4.988	4.983	4.980	5.245	5.162	5.116	5.111
t_2b	5.340	5.367	5.446	5.441	5.457	4.826	4.962	4.935	4.919	5.113	5.248	5.333	5.344	5.690	5.713	5.651	5.676	5.641	5.675	5.608	5.599
t_2c	6.561	5.906	6.044	6.048	6.073	**4.994**	**5.144**	**5.138**	**5.119**	**5.409**	**5.665**	**5.738**	**5.779**	6.064	6.115	6.017	6.047	5.909	6.037	5.980	**5.922**
t_2d	5.898	5.314	5.444	5.438	5.454	5.269	5.472	5.602	5.641	5.249	5.409	5.438	5.452	5.651	5.699	5.608	5.611	5.746	5.760	5.725	5.705
t_2e	5.648	5.188	5.322	5.316	5.329	5.632	5.797	5.960	6.004	5.215	5.354	5.362	5.384	5.533	5.471	5.392	5.420	5.705	5.676	5.633	5.576
t_2f	5.704	5.007	5.298	5.287	5.302	4.835	5.035	5.101	5.119	4.959	5.246	5.389	5.408	5.672	5.663	5.633	5.714	5.630	5.676	5.592	5.581
onc[b]		6	6	6	6	7	7	7	7	5	6	6	6	5	5	5	5	5	5	5	5
$SDEP_{cv}$[c]		0.453	0.419	0.415	0.413	0.447	0.389	0.362	0.355	0.420	0.353	0.333	0.328	0.427	0.338	0.322	0.319	0.414	0.324	0.308	0.295
$SDEP_{pred}$[d]		0.392	0.350	0.349	0.345	0.606	0.554	0.543	0.569	0.549	0.458	0.427	0.411	0.436	0.414	0.421	0.419	0.453	0.364	0.365	0.376
R^2_{pred}[e]		0.641	0.714	0.716	0.722	0.143	0.284	0.311	0.244	0.297	0.510	0.574	0.606	0.557	0.600	0.586	0.589	0.521	0.690	0.688	0.670
P^2[f]		0.745	0.788	0.786	0.790	0.415	0.474	0.446	0.403	0.658	0.706	0.692	0.700	0.628	0.629	0.631	0.621	0.558	0.690	0.699	0.687

[a] Shown are the results obtained from the five models with highest internal Q^2. Marked in bold are predictions that were considered as outliers because they deviated by more than 2 standard deviations ($SDEP_{cv}$) of the internal model. [b] Optimal number of components from leave out of random groups. [c] Standard deviation of prediction from leave out random groups calculated with eq 1. [d] Standard deviation of predictions for the external test set calculated with eq 2. [e] Q^2 for the external test set. [f] P^2 for the external test set calculated with eq 3.

Table 6. Predictions for the External Test Set by CoMFA Models Based on the Steric, HINT, or Both Fields Additionally Including Lipophilicity as a Scalar Variable[a]

		steric & logP				steric & HlogP				HINT & HlogP				Both & logP				Both & HlogP			
compd	obsd	0 FFD	1 FFD	2 FFD	3 FFD	0 FFD	1 FFD	2 FFD	3 FFD	0 FFD	1 FFD	2 FFD	3 FFD	0 FFD	1 FFD	2 FFD	3 FFD	0 FFD	1 FFD	2 FFD	3 FFD
t_1b	6.314	6.178	6.230	6.199	6.423	6.336	6.430	6.399	6.373	6.039	6.034	6.042	6.101	6.197	6.186	6.214	6.222	6.309	6.365	6.374	6.403
t_1c	5.577	5.540	5.591	5.552	5.603	5.450	5.629	5.599	5.638	5.567	5.554	5.561	5.598	5.820	5.803	5.858	5.856	5.824	5.903	5.887	5.915
t_1d	6.042	6.040	6.085	6.034	6.162	6.167	6.218	6.150	6.167	5.976	5.974	5.972	6.008	6.081	6.058	6.055	6.064	6.206	6.233	6.226	6.195
t_1f	6.602	6.318	6.440	6.412	6.163	5.980	6.211	6.142	6.065	5.871	6.021	6.028	6.072	6.138	6.143	6.144	6.129	**5.824**	**5.843**	**5.834**	**5.846**
t_1g	5.740	5.864	5.901	5.854	5.975	5.930	6.018	5.953	5.925	5.810	5.809	5.801	5.825	5.960	5.943	5.944	5.974	6.055	6.096	6.081	6.101
t_1k	6.745	6.461	6.371	6.411	6.564	6.525	6.531	6.540	6.540	6.616	6.545	6.554	6.546	6.317	6.490	6.447	6.417	6.528	6.501	6.565	6.586
t_1l	7.301	6.741	6.707	6.746	7.020	6.944	6.981	6.996	6.964	6.533	**6.438**	**6.450**	**6.439**	6.769	6.939	6.931	6.965	7.066	7.060	7.166	7.214
t_3c	6.469	6.050	6.206	6.160	6.403	6.293	6.428	6.359	6.339	**5.554**	**5.611**	**5.578**	**5.540**	6.172	6.143	6.180	6.145	6.333	6.467	6.464	6.507
t_3f	6.956	6.764	6.684	6.731	6.993	6.926	6.947	6.966	6.933	6.814	6.758	6.744	6.749	6.545	6.699	6.686	6.731	6.893	6.853	6.952	6.974
t_3g	6.921	6.496	6.425	6.469	6.668	6.611	6.636	6.647	6.631	6.593	6.512	6.514	6.545	6.382	6.547	6.507	6.516	6.679	6.634	6.706	6.736
t_3i	6.678	6.332	6.288	6.327	6.673	6.603	6.636	6.650	6.640	6.653	6.589	6.609	6.600	6.440	6.620	6.589	6.644	6.889	6.879	6.992	7.035
t_5a	5.189	6.010	**6.106**	**6.040**	**6.098**	5.992	**6.123**	**6.060**	**6.047**	5.781	5.888	5.870	5.862	**6.206**	**6.181**	**6.221**	**6.125**	**6.064**	**6.114**	**6.108**	**6.140**
t_5b	5.597	5.880	5.987	5.918	5.983	5.866	6.015	5.946	5.923	6.057	6.174	6.158	6.151	6.066	6.029	6.052	5.981	5.919	5.957	5.940	5.983
t_6a	5.991	6.597	6.633	6.566	6.415	6.350	6.449	6.405	6.368	6.246	6.351	6.347	6.329	6.604	6.573	6.608	6.612	6.184	6.314	6.294	6.334
t_6b	7.046	6.981	7.066	7.044	6.865	6.809	6.861	6.837	6.748	6.577	6.566	6.559	6.538	6.933	6.949	6.987	7.007	6.589	6.588	6.586	6.642
t_6c	5.983	6.289	6.305	6.267	6.159	6.134	6.114	6.171	6.163	5.918	6.032	6.031	6.019	6.118	6.049	6.110	6.157	6.077	6.174	6.152	6.106
t_2a	4.752	5.552	5.500	**5.498**	4.837	4.863	4.767	4.802	4.830	4.758	4.878	4.883	4.915	5.436	5.464	5.487	5.471	4.788	4.883	4.838	4.853
t_2b	5.340	5.798	5.887	5.828	5.658	5.579	5.686	5.624	5.656	5.143	5.124	5.101	5.097	5.910	5.857	5.834	5.809	5.649	5.737	5.724	5.774
t_2c	6.561	6.269	6.391	6.330	6.619	6.569	6.647	6.587	6.546	5.993	5.880	5.856	5.870	6.396	6.366	6.364	6.311	6.628	6.725	6.744	6.807
t_2d	5.898	6.027	6.139	6.091	5.905	5.866	5.919	5.892	5.931	5.616	5.631	5.621	5.663	6.057	6.019	6.002	5.931	5.798	5.895	5.858	5.891
t_2e	5.648	6.033	6.122	6.081	5.734	5.739	5.783	5.725	5.741	5.746	5.895	5.882	6.030	5.984	5.923	5.896	5.855	5.686	5.786	5.766	5.764
t_2f	5.704	5.678	5.681	5.605	**6.438**	6.464	6.413	6.381	**6.509**	6.525	**6.502**	**6.493**	**6.551**	6.080	5.996	6.055	5.982	**6.718**	**6.902**	**6.885**	**6.952**
onc[b]		6	6	6	6	7	6	6	5	5	6	6	6	4	4	4	5	6	5	5	5
$SDEP_{cv}$[c]		0.449	0.395	0.374	0.374	0.427	0.379	0.372	0.364	0.411	0.382	0.376	0.368	0.400	0.350	0.345	0.338	0.380	0.326	0.315	0.314
$SDEP_{pred}$[d]		0.39	0.414	0.386	0.326	0.327	0.335	0.315	0.335	0.435	0.459	0.460	0.466	0.435	0.390	0.404	0.406	0.384	0.431	0.423	0.438
R^2_{pred}[e]		0.645	0.599	0.652	0.752	0.751	0.738	0.769	0.737	0.558	0.507	0.506	0.492	0.557	0.645	0.619	0.653	0.655	0.566	0.583	0.552
P^2[f]		0.649	0.613	0.658	0.778	0.755	0.766	0.784	0.750	0.592	0.533	0.534	0.511	0.569	0.663	0.640	0.670	0.687	0.605	0.629	0.618

[a] Shown is the effect of variable selection before (0 FFD) and after 1−3 FFD runs. Marked in bold are predictions that were considered as outliers because they deviated by more than 2 standard deviations ($SDEP_{cv}$) of the internal model. [b] Optimal number of components from leave out of random groups. [c] Standard deviation of prediction from leave out random groups calculated with eq 1. [d] Standard deviation of predictions for the external test set calculated with eq 2. [e] Q^2 for the external test set. [f] P^2 for the external test set calculated with eq 3.

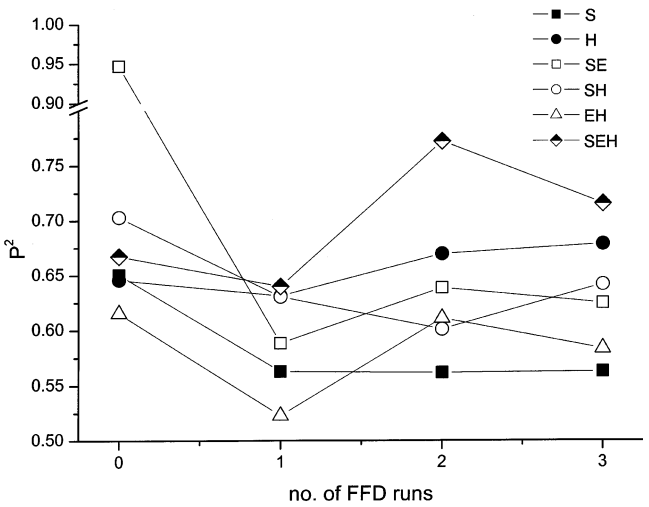

Figure 6. External predictivity of the CoMSIA models as measured by P^2 after different runs of variable selection by FFD. Abbreviations are the following: S (steric), E (electrostatic), H (hydrophobic) CoMSIA fields. The electrostatic field is omitted because it yielded negative P^2 values.

reported in the later work of Ecker et al. To include the four compounds (**1b**−**d**,**g**) from ref 14 that were mentioned only in this paper, their log(1/IC_{50}) values were fitted to the other data by linear regression based on the high correlation ($r^2 = 0.969$) observed for 14 overlapping derivatives for which multiple activity data were available.

For seven structurally diverse benzofurane derivatives (**1f** and **2a**−**f**), only inhibition of rhodamine-123 efflux had been reported in ref 15. As for 12 other derivatives, inhibition of both daunomycin and rhodamine-123 had been reported, which proved to be highly correlated ($r^2 = 0.968$). Again, the missing values were calculated by linear regression. This allowed the inclusion of additional and structurally deviating derivatives. To give no priority to the daunomycin or the rhodamine-123 values, two regressions were performed, using either of them as a dependent variable and averaging the calculated daunomycin log(1/IC_{50}) values.

We divided the available data into training and external test sets to investigate the effect of variable selection on external predictivity. For the selection of which compounds should form the external test set, basically two strategies can be used: (1) clustering of the derivatives according to structural similarity and then picking of test set members from the clusters; (2) a kind of random selection. We used the latter approach because the selection based on similarity would yield a test set too similar to the training set. Therefore, we decided to select the 48 derivatives for which data had been reported in ref 11 as a training set, leaving 22 other compounds for the external test set. This selection can be regarded as a rather hard test of the external predictivity because of the structurally deviating benzofuranes being in the test set only. However, these derivatives can be easily overlaid with the other derivatives and do not occupy space in 3D uncovered by the training set.

Table 1 shows the structures and IC_{50} values of the compounds studied. The HINT and logP values reported by Ecker et al. are also included because they were used as an additional descriptor in the 3D-QSAR studies. In the table, the same codes of the compounds are used as in the source papers and the test set compounds are preceded by "**t_**".

Optimization and Alignment of the Structures. The conformations of the previously studied 28 derivatives were taken from ref 3 and were used without modification. The structures of the remaining compounds were generated by modification of closely related structures followed by energy minimization. For the compounds **t_6a**, **t_6b**, and **8**, a systematic conformational search around the flexible nitrogen substituent was performed. From the extracted local energy minima, selections were those that showed the best overlap of the aromatic rings, with the other derivatives possessing also an aromatic nitrogen substituent.

The alignment of all derivatives was based on the Ar−Ar−N alignment used in our previous study of the smaller subset of propafenone derivatives.[3] In this alignment rule, the centroids of both aromatic rings and the basic nitrogen are overlaid. The structures having no second aromatic ring (**18**, **19**, **25**−**27**, **41**−**43**, **46**−**48**, **t_2a**) were aligned on the carbon atoms of the benzene ring and the basic nitrogen. In that case, the weight of the nitrogen in the fitting was increased to 6 in order to equally contribute to the alignment.

Computational Approaches. The initial CoMFA and CoMSIA[16,17] models were calculated with the SYBYL 6.5 molecular modeling software.[18] For the calculation of charges, the AM1 Hamiltonian was used as implemented in MOPAC 6 and supplied by SYBYL. The HINT (Hydropatic INTeraction) program[19,20] was used for the calculation of the hydrophobic fields used in CoMFA. Two types of hydrophobic fields were considered because both of them had been shown to give superior results in previous CoMFA analyses:[3,4] the standard hydrophobic field (H) and the hydrophobic only field (Ho) where negative (hydrophilic) values are truncated to zero. The following standard characteristics were used to calculate the CoMFA and CoMSIA fields: 2 Å regular grid spacing in all three dimensions within the defined region; 4 Å extension of the region beyond the van der Waals volume of the molecules; an sp^3 carbon probe atom with +1 charge; a distance-dependent dielectric constant. The same region was used in all calculations. As in the SYBYL implementation of CoMFA, different results were obtained when steric and electrostatic fields were computed together (B, both field) or separately and later combined (S&E, steric and electrostatic); both methods of calculation were included. This difference is due to the fact that in case of the B field the electrostatic field is assigned a missing value inside atoms and therefore is ignored at these points, while when the electrostatic field is calculated separately, points inside atoms are set to the selected cutoff and are subsequently taken into account in the PLS analysis.

For the CoMSIA fields, the default settings were used. In addition to the steric and electrostatic fields, the hydrophobic field was considered. For the calculation of the hydrophobic CoMSIA fields, atomic values that are directly based on the research of Viswanadhan et al.[21] are used.

The GOLPE procedure (generating optimal linear PLS estimations) is a method for detecting variables that increase the predictivity of PLS models.[22] In the data pretreatment, very small X values below 0.01 were converted to zero with the zeroing option. A minimum standard deviation of 0.2 was used to remove variables with very low variance. BUW scaling (block unscaled weight) was used in the case of combined fields to normalize the variance of each block (field), thus giving the same importance to each field.

The initial PLS models were developed by setting the maximal dimensionality to the optimum number of components obtained from the initial PLS calculation with SYBYL plus 1. This setting was chosen to ensure that the optimal model was included. The models were validated by cross-validation using both leave-one-out and leave-N-out with six random groups. Each of these groups was omitted from the data set at a time, and a reduced PLS model was built with the remaining compounds. The whole procedure was repeated 20 times, the default value within GOLPE. This cross-validation scheme is expected to yield a more realistic estimate of the predictivity of the PLS model than the usual leave-one-out procedure. During the cross-validation, the weights were recalculated each time. This is a time-consuming process, but the calculation is more accurate. The quality of the 3D-QSAR models was estimated with two methods: best Q^2 and best $SDEP_{cv}$ values. For the calculation of $SDEP_{cv}$, basically two formulas are used in the literature that differ slightly. For the estimation of the optimal number of components (N_{opt}), the following formula was used:

Table 7. Predictions for the External Test Set by Different CoMSIA Models before (0) and after 1−3 FFD Runs[a]

		steric				hydrophobic				steric & hydrophobic				steric & electrostatic				steric & electrostatic & hydrophobic			
compd	obsd	0 FFD	1 FFD	2 FFD	3 FFD	0 FFD	1 FFD	2 FFD	3 FFD	0 FFD	1 FFD	2 FFD	3 FFD	0 FFD	1 FFD	2 FFD	3 FFD	0 FFD	1 FFD	2 FFD	3 FFD
t_1b	6.314	6.016	6.112	6.075	6.110	5.925	6.248	6.077	6.084	5.955	6.155	6.223	6.136	6.060	6.253	6.148	6.180	5.969	6.119	6.031	6.098
t_1c	5.577	5.375	4.743	4.738	4.817	5.667	5.937	5.826	5.835	5.462	5.752	5.805	5.707	5.629	5.903	5.737	5.769	5.745	5.860	5.823	5.853
t_1d	6.042	5.680	5.467	5.455	5.510	5.952	6.142	6.039	6.042	5.748	5.933	5.993	5.914	5.887	6.219	6.074	6.101	5.982	6.106	6.067	6.188
t_1f	6.602	5.856	5.913	5.911	5.928	6.407	6.611	6.533	6.514	6.538	6.681	6.758	6.715	6.593	**5.700**	**5.618**	**5.623**	6.057	6.103	6.082	6.083
t_1g	5.740	5.741	5.685	5.673	5.710	5.862	6.036	5.947	5.950	5.850	5.888	5.973	5.882	5.975	6.176	6.057	6.077	5.922	6.028	5.976	5.993
t_1k	6.745	6.201	6.151	6.177	6.187	6.468	6.671	6.631	6.633	6.448	6.461	6.461	6.466	6.684	6.427	6.350	6.346	6.257	6.275	6.498	6.397
t_1l	7.301	6.394	6.644	6.652	6.642	**6.399**	**6.467**	**6.403**	**6.395**	**6.389**	**6.433**	**6.415**	**6.418**	7.069	**6.298**	**6.264**	**6.260**	**6.275**	**6.289**	**6.526**	**6.421**
t_3c	6.469	5.915	6.158	6.119	6.108	5.744	5.828	5.723	**5.707**	5.796	5.976	5.995	5.866	6.264	6.205	6.067	6.082	5.955	6.015	5.766	**5.707**
t_3f	6.956	6.666	7.141	7.148	7.151	6.590	6.765	6.742	6.756	6.693	6.712	6.713	6.796	7.119	6.492	6.504	6.510	6.514	6.481	6.638	6.620
t_3g	6.921	6.182	6.166	6.190	6.199	6.509	6.634	6.596	6.600	6.476	6.513	6.514	6.534	6.868	6.391	6.342	6.342	6.358	6.392	6.619	6.547
t_3i	6.678	6.285	6.382	6.404	6.416	6.432	6.514	6.472	6.469	6.420	6.437	6.433	6.447	6.764	6.356	6.327	6.325	6.360	6.362	6.579	6.523
t_5a	5.189	5.599	5.525	5.508	5.531	5.719	5.885	5.602	5.609	5.629	5.942	5.933	5.814	5.357	5.639	5.479	5.492	5.659	5.725	5.531	5.457
t_5b	5.597	5.559	5.451	5.435	5.453	5.761	5.974	5.682	5.694	5.688	5.983	5.987	5.880	5.389	5.692	5.535	5.548	5.688	5.759	5.584	5.547
t_6a	5.991	6.010	6.143	6.344	6.327	6.627	**6.866**	**6.777**	6.744	6.469	**6.811**	**6.848**	**6.824**	6.065	5.707	5.669	5.668	6.149	6.196	6.144	6.256
t_6b	7.046	6.241	6.635	6.708	6.648	6.675	6.753	6.762	6.747	6.587	6.754	6.756	6.685	7.226	6.583	6.472	6.489	6.497	6.640	6.590	6.658
t_6c	5.983	6.380	6.403	6.449	6.428	6.204	6.356	6.282	6.284	6.149	6.364	6.415	6.334	6.122	6.413	6.256	6.271	6.186	6.197	6.086	6.295
t_2a	4.752	4.731	3.983	3.937	3.930	5.211	5.109	5.124	5.034	5.071	4.908	5.040	4.869	4.853	4.701	4.455	4.443	5.012	5.041	4.660	4.710
t_2b	5.340	5.242	4.794	4.846	4.848	5.797	5.793	5.746	5.721	5.466	5.671	5.729	5.571	5.427	5.735	5.480	5.497	5.717	5.798	5.598	5.572
t_2c	6.561	5.476	**5.423**	**5.495**	**5.424**	6.419	6.403	6.497	6.454	6.129	6.246	6.359	6.213	6.574	5.934	**5.614**	**5.608**	6.167	6.314	6.068	5.963
t_2d	5.898	5.288	**4.826**	**4.896**	**4.889**	5.847	5.889	5.826	5.761	5.556	5.770	5.830	5.671	5.739	5.784	5.524	5.543	5.742	5.855	5.683	5.657
t_2e	5.648	5.451	5.472	5.396	5.422	5.899	5.991	5.961	5.908	5.942	6.042	6.197	6.066	5.815	5.924	5.701	5.732	5.804	5.985	5.807	5.787
t_2f	5.704	5.108	**4.773**	4.849	4.913	5.714	5.745	5.662	5.601	5.301	5.728	5.747	5.596	5.575	5.532	5.298	5.337	5.488	5.654	5.522	5.551
onc[b]		5	6	6	6	6	7	6	6	7	6	6	6	5	6	6	6	5	5	6	6
$SDEP_{cv}$[c]		0.504	0.436	0.432	0.429	0.426	0.398	0.384	0.378	0.443	0.390	0.375	0.370	0.460	0.421	0.399	0.393	0.436	0.376	0.356	0.348
$SDEP_{pred}$[d]		0.520	0.597	0.585	0.579	0.393	0.404	0.376	0.372	0.387	0.398	0.416	0.393	0.151	0.441	0.481	0.480	0.420	0.391	0.416	0.393
R^2_{pred}[e]		0.368	0.166	0.201	0.217	0.639	0.620	0.670	0.678	0.651	0.630	0.596	0.640	0.947	0.545	0.460	0.462	0.588	0.643	0.600	0.640
P^2[f]		0.651	0.563	0.562	0.563	0.646	0.631	0.670	0.679	0.703	0.631	0.601	0.642	0.947	0.588	0.639	0.625	0.668	0.644	0.601	0.642

[a] Marked in bold are predictions that were considered as outliers because they deviated by more than 2 standard deviations ($SDEP_{cv}$) of the internal model. [b] Optimal number of components from leave out of random groups. [c] Standard deviation of prediction from leave out random groups calculated with eq 1. [d] Standard deviation of predictions for the external test set calculated with eq 2. [e] Q^2 for the external test set. [f] P^2 for the external test set, calculated with eq 3.

$$\mathrm{SDEP} = \sqrt{\frac{(Y_{\mathrm{obs}} - Y_{\mathrm{pred}})^2}{n - c - 1}} \quad (1)$$

It corresponds to the formula used in SYBYL and takes into account the number of components used to build the model. In this way, the tradeoff between an increase in Q^2 and increasing model complexity due to increasing number of components is taken into account. The "best" model was taken as the one with the lowest $\mathrm{SDEP_{cv}}$. Because in GOLPE the number of components is calculated according to

$$\mathrm{SDEP} = \sqrt{\frac{(Y_{\mathrm{obs}} - Y_{\mathrm{pred}})^2}{n}} \quad (2)$$

which does not consider the number of components used to build the model and parallels Q^2, the $\mathrm{SDEP_{cv}}$ values from GOLPE were recalculated according to eq 1.

The estimation and comparison of the performance of the generated models require some caution. The calculation of Q^2 for an external test set is only suitable if the mean values of the training and test sets are identical or at least differ by not too much. Therefore, training and test set predictions were compared using eq 2. Compared to the use of eq 1, this is advantageous for the test set because otherwise the number of compounds in the test set and the number of components would influence and bias the result.

A few years ago, a new method was published by Silverman for the calculation of the quality of test set predictions.[23] This method avoids problems due to differences in the mean values of the training and test sets. A parameter called P^2 was defined according to

$$P^2 = 1 - \frac{\sum_{i,j}[(p_i - p_j) - (m_i - m_j)]^2}{\sum_{i,j}(m_i - m_j)^2} \quad (3)$$

where p_i and p_j are the predicted activities, m_i and m_j are the measured activity values of the external test set, and the summation runs over all pairs of compounds i and j in the test set. P^2 is based on pairwise predicted and observed activity differences. The advantage of P^2 is the fact that it is independent of additive constants such as the mean and equals Q^2 in the case of identical mean values of the test and training sets. Therefore, this measure of predictive performance was also calculated and considered.

The selection of the X variables was performed by applying first the smart region definition (SRD) followed by fractional factorial design (FFD). The selection of the seed variables for the SRD was based on the PLS weights of the X variables. The dimensionality was set to the optimal number of components based on the minimal SDEP value as obtained from the previous PLS analysis. The critical distance in grid units was left at its default value of 1, and collapsing of groups was allowed using a collapsing distance of two grid units. The number of seeds that are extracted from the X variables was increased to 50% of the X variables because in initial experiments we found that several X variables with high weights were not selected when using the default settings.

The fractional factorial design to identify contributing variables was performed with the default settings except that foldover design was used to evaluate the effect of the variables on the model predictivity in a more reliable fashion. Uncertain X variables, those contributions that could not be distinguished from the added dummy variables, were retained. This was done to avoid destroying the structure of the X variables. After FFD, the negatively contributing X variables were deleted and a new PLS model was generated.

The procedure of grouping of seeds followed by variable selection with FFD was repeated up to three times.

References

(1) Gottesmann, M. M. How cancer cells evade chemotherapy: sixteenth Richard and Hilda Rosenthal Foundation award lecture. *Cancer Res.* **1993**, *53*, 747−754.

(2) Martin, C.; Berridge, G.; Higgins, C. F.; Mistry, P.; Charlton, P.; Callaghan, R. Communication between Multiple Drug Binding Sites on P-glycoprotein. *Mol. Pharmacol.* **2000**, *58*, 624−632.

(3) Pajeva, I. K.; Wiese, M. A Comparative Molecular Field Analysis of Propafenone-Type Modulators of Cancer Multidrug Resistance. *Quant. Struct.−Act. Relat.* **1998**, *17*, 301−312.

(4) Pajeva, I. K.; Wiese, M. Molecular modeling of phenothiazines and related drugs as multidrug resistance modifiers: a comparative molecular field analysis study. *J. Med. Chem.* **1998**, *41*, 1815−1826.

(5) Klebe, G. Comparative molecular similarity indices analysis: CoMSIA. In *3D QSAR in Drug Design*; Kubinyi, H., Folkers, G., Martin, Y. C., Eds.; Kluwer Academic Publishers: Dordrecht, The Netherlands, 1998; Vol. 3, pp 87−104.

(6) Matter, H.; Schwab, W. Affinity and Selectivity of Matrix Metalloproteinase Inhibitors: A Chemometrical Study from the Perspective of Ligands and Proteins. *J. Med. Chem.* **1999**, *42*, 4506−4523.

(7) Gnerre, C.; Catto, M.; Leonetti, F.; Weber, P.; Carrupt, P.-A.; Altomare, C.; Carotti, A.; Testa, B. Inhibition of Monoamine Oxidase by Functionalized Coumarin Derivatives: Biological Activities, QSARs, and 3D-QSARs. *J. Med. Chem.* **2000**, *43*, 4747−4758.

(8) Poso, A.; Gynther, J.; Juvonen, R. A comparative molecular field analysis of cytochrome P450 2A5 and 2A6 inhibitors. *J. Comput.-Aided Mol. Des.* **2001**, *15*, 195−202.

(9) Nielsen, S. F.; Nielsen, E. O.; Olsen, G. M.; Liljefors, T.; Peters, D. Novel Potent Ligands for the Central Nicotinic Acetylcholine Receptor: Synthesis, Receptor Binding, and 3D-QSAR Analysis. *J. Med. Chem.* **2000**, *43*, 2217−2226.

(10) Cinone, N.; Höltje, H.-D.; Carotti, A. Development of a unique 3D interaction model of endogenous and synthtic peripheral benzodiazepine receptor ligands. *J. Comput.-Aided Mol. Des.* **2000**, *14*, 753−768.

(11) Tmej, C.; Chiba, P.; Huber, M.; Richter, E.; Hitzler, M.; Schaper, K.-J.; Ecker, G. A Combined Hansch/Free-Wilson Approach as Predicitve Tool in QSAR Studies on Propafenone-Type Modulators of Multidrug Resistance. *Arch. Pharm. (Weinheim, Ger.)* **1998**, *331*, 233−240.

(12) Chiba, P.; Hitzler, M.; Richter, E.; Huber, M.; Tmej, C.; Giovagnoni, E.; Ecker, G. Studies on Propafenone-Type Modulators of Multidrug Resistance III: Variations on the Nitrogen. *Quant. Struct.−Act. Relat.* **1997**, *16*, 361−366.

(13) Chiba, P.; Tell, B.; Jäger, W.; Richter, E.; Hitzler, M.; Ecker, G. Studies on Propafenone-Type Modulators of Multidrug-Resistance IV: Synthesis and Pharmacological Activity of 5-Hydroxy and 5-Benzyloxy Derivatives. *Arch. Pharm. (Weinheim, Ger.)* **1997**, *330*, 343−347.

(14) Chiba, P.; Ecker, G.; Schmid, D.; Drach, J.; Tell, B.; Goldenberg, S.; Gekeler, V. Structural Requirements for Activity of Propafenone-Type Modulators in P-Glycoprotein-Mediated Multidrug Resistance. *Mol. Pharmacol.* **1996**, *49*, 1122−1130.

(15) Ecker, G.; Chiba, P.; Hitzler, M.; Schmid, D.; Visser, K.; Cordes, H.-P.; Csöllei, J.; Seydel, J. K.; Schaper, K.-J. Structure−Activity Relationship Studies on Benzofuran Analogs of Propafenone-Type Modulators of Tumor Cell Multidrug Resistance. *J. Med. Chem.* **1996**, *39*, 4767−4774.

(16) Klebe, G.; Abraham, U.; Mietzner, T. Molecular similarity indices in a comparative analysis (CoMSIA) of drug molecules to correlate and predict their biological activity. *J. Med. Chem.* **1994**, *37*, 4130−4146.

(17) Klebe, G. Comparative molecular similarity indices analysis: CoMSIA. *Perspect. Drug Discovery Des.* **1998**, *12−14*, 87−104.

(18) Tripos Associates, 1699 Hanley Road, St. Louis, MO 63144.

(19) Kellogg, G. E.; Semus, S. F.; Abraham, D. J. HINT: A new method for empirical hydrophobic field calculation for CoMFA. *J. Comput.-Aided Mol. Des.* **1991**, *5*, 545−552.

(20) Edusoft, LC, P.O. Box 1811, Asland, VA 23005.

(21) Viswanadhan, V. N.; Ghose, A. K.; Revankar, G. R.; Robins, R. K. Atomic Physicochemical Parameters for Three-Dimensional Structure Directed Quantitative Structure−Activity Relationships. 4. Additional Parameters of Hydrophobic and Dispersive Interactions and Their Application for an Automated Superposition of Certain Naturally Occurring Nucleoside Antibiotics. *J. Chem. Inf. Comput. Sci.* **1989**, *29*, 163−172.

(22) *GOLPE*, version 4.5; Multivariate Infometric Analysis Srl., Viale dei Castagni 16: Perugia, Italy, 1999.

(23) Silverman, D. The thirty-one benchmark steroids revisited: comparative molecular moment analysis (CoMMA) with principal component regression. *Quant. Struct.−Act. Relat.* **2000**, *19*, 237−246.

JM030876R